Nuclear Science and Techniques (2025) 36:32
https://doi.org/10.1007/s41365-024-01606-y

Reconstruction of pile-up events using a one-dimensional convolutional autoencoder for the NEDA detector array

J. M. Deltoro[1] · G. Jaworski[2] · A. Goasduff[3] · V. González[1] · A. Gadea[4] · M. Palacz[2] · J. J. Valiente-Dobón[3] · J. Nyberg[5] · S. Casans[1] · A. E. Navarro-Antón[1] · E. Sanchis[1] · G. de Angelis[3] · A. Boujrad[6] · S. Coudert[6] · T. Dupasquier[7] · S. Ertürk[8] · O. Stezowski[7] · R. Wadsworth[9]

Received: 24 July 2024 / Revised: 24 September 2024 / Accepted: 9 October 2024 / Published online: 12 January 2025

Abstract
Pulse pile-up is a problem in nuclear spectroscopy and nuclear reaction studies that occurs when two pulses overlap and distort each other, degrading the quality of energy and timing information. Different methods have been used for pile-up rejection, both digital and analogue, but some pile-up events may contain pulses of interest and need to be reconstructed. The paper proposes a new method for reconstructing pile-up events acquired with a neutron detector array (NEDA) using an one-dimensional convolutional autoencoder (1D-CAE). The datasets for training and testing the 1D-CAE are created from data acquired from the NEDA. The new pile-up signal reconstruction method is evaluated from the point of view of how similar the reconstructed signals are to the original ones. Furthermore, it is analysed considering the result of the neutron-gamma discrimination based on charge comparison, comparing the result obtained from original and reconstructed signals.

Keywords 1D-CAE · Autoencoder · CAE · Convolutional neural network (CNN) · Neutron detector · Neutron-gamma discrimination (NGD) · Machine learning · Pulse shape discrimination · Pile-up pulse

1 Introduction

Pulse pile-up is a common problem in nuclear reaction and spectroscopy experiments with high counting rates. The pulse pile-up effect happens when pulses arrive close in time so that both pulses are totally or partially overlapping. Due to the overlap, the two pulses are distorted, as shown in Fig. 1. This effect degrades the quality of energy and timing information, making it difficult to identify particle types using pulse shape discrimination techniques [1–3]. For this reason, these types of events are usually rejected.

This work was partially supported by MICIU MCIN/AEI/10.13039/501100011033, Spain with grant PID2020-118265GB-C42,-C44, PRTR-C17.I01, by Generalitat Valenciana, Spain with grant CIPROM/2022/54, ASFAE/2022/031, CIAPOS/2021/114 and by the EU NextGenerationEU, ESF funds, and the National Science Centre (NCN), Poland (grant No. 2020/39/D/ST2/00466).

✉ J. M. Deltoro
josemadeltoro@gmail.com

[1] Department of Electronic Engineering, University of Valencia, Burjassot, Valencia, Spain

[2] Heavy Ion Laboratory, University of Warsaw, 02-093 Warsaw, Poland

[3] Istituto Nazionale di Fisica Nucleare, Laboratori Nazionali di Legnaro, Legnaro, Italy

[4] Instituto de Física Corpuscular, CSIC-Universidad de Valencia, 46980 Paterna, Valencia, Spain

[5] Department of Physics and Astronomy, Uppsala University, Uppsala, Sweden

[6] GANIL, CEA/DRF-CNRS/IN2P3, Bvd. Henri Becquerel, 14076 Caen, France

[7] CNRS, IN2P3, IPN Lyon, Université Lyon 1, 69622 Villeurbanne, France

[8] Department of Physics, Nigde Omer Halisdemir University, 51240 Nigde, Turkey

[9] Department of Physics, University of York, Heslington, York YO10 5DD, UK

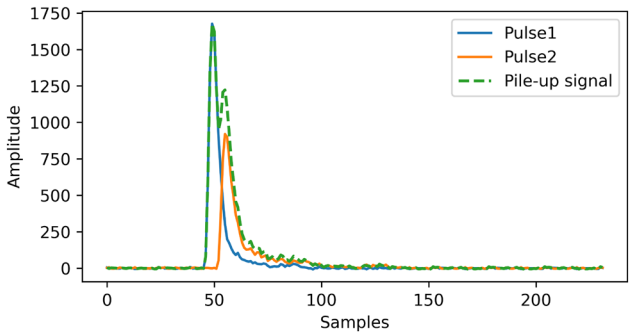

Fig. 1 Example of a signal with pulse pile-up effect

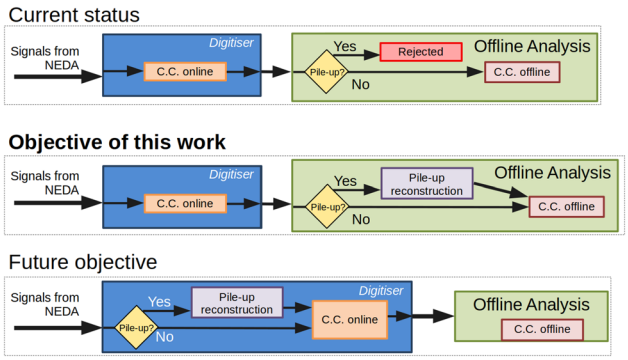

Fig. 2 Current status rejects the pile-up signals. The objective of this work is the development of a method for reconstructing offline pile-up signals. In the future it will be included in online signal processing

Different techniques have been conceived to detect consecutive pulses to reject or eliminate this type of signal. Some of them are based on digital and analogue methods like leading-edge discrimination, moment-analysis, CFD (Constant-Fraction Discrimination), DCFD (Digital Constant-Fraction Discrimination), triangular pulse shaping with a leading-edge linear regression, and pulse shape fitting, which were studied in [4, 5]. Also, other methods like analogue circuits [6], trapezoidal shaping [7], methods based on Position Shift Identification [5], methods using PSD [8], Neural Networks [9], and even ASIC (Application-Specific Integrated Circuits) [10] have been used for pile-up rejection.

However, some of the events rejected by these techniques contain information that may be of interest. Therefore, there are also some methods to recover this information from two or more pile-up pulses. These methods can be grouped into techniques focusing on refining the distorted pulse height spectrum [11, 12] or individually treating the signals. Among the latter, some techniques focus on obtaining pulse height information [13], while others focus on determining the type of particles to which each pile-up pulse corresponds using pulse shape discrimination methods and machine learning techniques [14–16].

Nevertheless, for some applications or experiments, the information of the two pile-up pulses is needed, so a complete reconstruction of both pulses is necessary. There are no general solutions in these pulse reconstructions that can be used for all applications. Therefore, specific solutions have been developed for particular cases, such as the fitting and extrapolation method [17–19] or the deconvolution method [20].

For example, two methods have been developed for reconstructing pile-up events acquired with organic scintillators. The first method, based on pile-up model comparison [21], is intended for offline use. It involves multiple iterations to fit one of the pile-up models to the acquired signals. The second method employs machine learning techniques [22] and can reconstruct pulses, although limited to those separated by more than 60 ns.

This paper studies a method aiming at achieving in a future an online pile-up event reconstruction, recovering the pulses with a time difference between pulses greater than or equal to 15 ns (3 samples @200 MHz). For this to be feasible, analytical and computational complexity must be low, and the reconstruction time per event should also be low to integrate the method into the overall analysis system. As a first step, the reconstruction method is implemented offline to check the feasibility, as shown in Fig. 2.

The reconstruction techniques mentioned before meet all the necessary requirements and, thus, cannot be used for (Neutron Detector Array) NEDA events. Therefore, this paper proposes an ad-hoc method using a 1D-CAE to disentangle the two pulses composing each pile-up event acquired with NEDA detectors [23].

The rest of the paper is organised as follows: Sect. 2 explains the pile-up effect specifically in NEDA, Sect. 3 describes the 1D-CAE architecture used for the pile-up event reconstruction, Sect. 4 explains the data acquisition and how the dataset is created for training and testing the 1D-CAE model, Sect. 5 shows the analyses of the reconstructed signals and the results obtained, and Sect. 6 presents the conclusions.

2 Pile-up in NEDA detector

NEDA is a neutron detector responsible for determining the reaction channel by measuring the number of neutrons emitted from the compound nuclei when working with a gamma-ray spectrometer. The NEDA array is based on individual hexagonal cells filled with ~ 3.15 L of liquid organic scintillator (ELJEN EJ301). This kind of detector exhibits sensitivity to neutrons, X-rays, and gamma rays. While X-rays can be effectively attenuated by shielding the detectors, this

approach proves impractical for higher-energy gamma rays, as it would compromise the efficiency of neutron detection. Given this unique characteristic of the detectors, it becomes essential to develop techniques for discriminating between gamma ray and neutron events (NGD) to determine the radiation's type. In NEDA, PSA (Pulse Shape Analysis) based on CC (Charge Comparison) and TOF (Time-of-Flight) information is used for NGD.

However, when two pulses are generated very close in time by the same NEDA cell, the pile-up effect occurs, and the event is typically discarded since reliable CC information cannot be obtained. Since the detector only reacts to gammas and neutrons, it gives rise to four possible combinations of pile-up: neutron-neutron, neutron-gamma, gamma-neutron, gamma-gamma.

Nevertheless, not all four combinations are equally likely or can be detected as pile-up signals. The neutron-neutron combination, i.e. two neutrons arriving at the same detector, has low the probability of occurring, and the time difference will be less than 5 ns. The analysis will identify it as a single neutron, i.e. pile-up will not be detected. The gamma-gamma combination is more likely to happen. However, if two gammas arrive at the same detector after the reaction, they will arrive simultaneously and be identified as a single gamma. The neutron-gamma combination, on the other hand, is likely to occur when a neutron is detected first, and then a spurious gamma is acquired from natural background radiation. This gamma can appear at any moment of the acquired signal. Finally, pile-up gamma-neutron events can occur when gammas from the reaction are detected arriving in the first nanoseconds, and later, the neutron arrives. Depending on the distance of the detectors from the reaction, a longer or shorter TOF will be obtained. With the standard NEDA installation, a distance of 100 cm is foreseen, resulting in an average flight time of neutrons of 40 ns. Given these characteristics in detection and acquisition, the pile-up reconstruction will focus exclusively on gamma-neutron or neutron-gamma events.

3 1D-CAE architecture for NEDA pile-up event reconstruction

Signals with pile-up must be reconstructed and treated in the same way as signals without pile-up; therefore, the pile-up problem is approached as a time series problem in which single dimension data are separated and reconstructed. This study focuses on solving the pile-up problem using a one-dimensional convolutional autoencoder (1D-CAE).

A 1D-CAE combines the principles of both a one-dimensional convolutional neural network (1D-CNN) [24] and an autoencoder [25]. It utilises convolutional layers for feature extraction and encoding of sequential data, followed by decoding layers to reconstruct the input sequence. The architecture of a 1D-CAE typically consists of an encoder module, which applies one-dimensional convolutional filters to reduce the dimensionality of the input sequence, and a decoder module, which employs transpose convolutional layers to upsample and reconstruct the original sequence. The loss function used in training the 1D-CAE compares the input sequence with the reconstructed output sequence. The two main concepts of the architecture, 1D-CNN and autoencoder, are explained below, followed by the specific architecture used to reconstruct pile-up events.

3.1 1D-CNN

A 1D-CNN [24] is a specialised neural network architecture designed to analyse sequential data such as time series, signals, or text sequences. Unlike traditional CNN's [26] that operate on two-dimensional grids like images, 1D-CNN's process data along a single dimension, making them well-suited for tasks where the ordering of elements matters.

The fundamental operation in a 1D-CNN is the convolutional layer. Here, the network learns to detect patterns or features within the input sequence by convolving it with learnable filters. Following the convolutional layers, pooling layers are often employed to reduce the dimensionality of the feature maps and capture the most important information. Max pooling, for instance, selects the maximum value within a fixed window and discards the rest. Additionally, activation functions like Rectified Linear Unit (ReLU) are applied after convolution and pooling operations to introduce nonlinearity into the network, enabling it to learn complex relationships in the data. Finally, one or more fully connected layers may be utilised to perform classification or regression tasks based on the features learned by the convolutional layers.

1D-CNN's can be applied to time series prediction of data, such as electrocardiogram (ECG) time series [27] or weather forecast [28]. They are also used in automatic speech recognition (ASR) [29], natural language processing, and signal identification.

3.2 Autoencoder

An autoencoder [25, 30] is a neural network architecture used in machine learning and pattern recognition. It comprises two main components: an encoder and a decoder. The encoder compresses the input into a lower-dimensional representation. It reduces the dimensionality of the input data and captures the most important features. Subsequently, the decoder takes this lower-dimensional representation and tries to produce an output as close as possible to the original input. This entails employing a loss function that compares the decoder's output with the corresponding input, enabling

the model to learn to reconstruct input data. The expression describing a autoencoder is:

$$L(x, x') = L(x, g(f(x))) \tag{1}$$

where

- L denotes the loss function comparing the original input x with the reconstruction x' or $g(f(x))$
- f represents the encoder function that maps the input x to a lower-dimensional representation space.
- g represents the decoder function that reconstructs the original input from the lower-dimensional representation obtained by the encoder.

There are various autoencoders, each designed to tackle different challenges in machine learning. Traditional autoencoders, also known as densely connected autoencoders, are versatile and commonly used for tasks such as dimensionality reduction and data reconstruction. Convolutional autoencoders [31] are ideal for image reconstruction, as they effectively leverage convolutions to capture spatial patterns. Others, such as variational autoencoders [32], are focused on generating new data, and denoising autoencoders [33] are robust models against noisy data.

3.3 1D-CAE architecture and training

As previously mentioned, the pile-up signals under study are composed of two pulses that occur very close together in time. As shown in Fig. 3, the proposed 1D-CAE architecture has one input, which is the signal with the two pile-up pulses, and two outputs, one output for each pulse of which the input signal is composed. For this, the encoder structure is common, and the decoder is separated in two, thus having a decoder for each of the reconstructed pulses.

In this way, with a single model, both pulses can be obtained separately and integrated directly into the processing chain. This approach allows for integration into future NEDA hardware and firmware upgrades without affecting the rest of the processing chain.

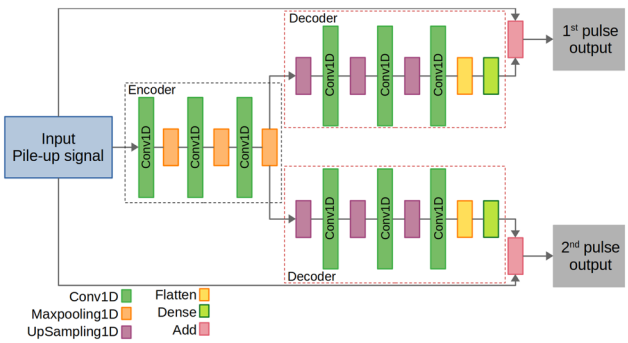

Fig. 3 1D-CAE architecture for NEDA pile-up event reconstruction

Figure 3 shows the 1D-CAE architecture that comprises several Convolutional 1D (Conv1D) layers, with a kernel size of 3, followed by MaxPooling1D layers, which reduce the dimensionality of the data. UpSampling1D layers are then used to increase the dimensionality again. Finally, Dense layers are used to flatten the data and connect it to the final outputs.

The first layer is connected to a 1D Convolutional layer with five channels and a ReLU trigger function. A MaxPooling1D layer with a reduction factor of 2 follows this layer. The same structure (Conv1 + MaxPooling1D) is then repeated twice more.

After this, the architecture is split into two decoder branches from a MaxPooling1D layer. Each branch has 3 Upsampling1D layers followed by 3 Conv1D layers with 20, 10 and 5 channels, respectively.

Following, branches are connected to two Flatten layers and then to dense layers with a ReLU activation function. An Add layer is used as a skip connection to sum the values with the input. The skip connection facilitates the direct flow of information from input to output layers, allowing the network to access the raw, unprocessed information. Finally, the two outputs are obtained.

The computational complexity of this model is 1.9 MFLOPS, which is relatively low, especially when compared to more advanced devices like the Versal Adaptive SoC [34], which operates in the GFLOP range. Given this low computational complexity, the model could be implemented on a microcontroller with a Floating Point Unit, such as the STM32L4 series with an Arm Cortex-M4 (capable of up to 80 MFLOPS at 80 MHz [35]). This makes it feasible for integration into future NEDA electronics without significantly increasing the computational load.

Once the 1D-CAE was developed, it was trained with artificial pile-up signals. The input signals are the artificial pile-up signals, and the expected output signals (ground truth) are the two signals from which the artificial pile-up signal was generated. The data acquisition process and creation of the artificial pile-up signals are described in the following section.

4 Dataset preparation

The artificial pile-up signals (neutron-gamma and gamma-neutron combinations) for training and testing were generated following these steps:

1. Acquiring from NEDA detectors.
2. Selecting and taking signals without pile-up.

3. Removing the baseline of the signals. This aids in pulse analysis and allows acquired pulses from different channels to be summed.
4. Analyse them to determine what type of event they represent (gamma or neutron) using the CC method.
5. Take two signals of different types.
6. One of them is shifted a distance of between 3 and 40 samples.
7. Finally, they are added together, generating the final pile-up signal.

By performing these steps, two datasets with artificial pile-up signals were created in which the origin of the signals composing the pile-up signal is known. Thus, pile-up signals with neutron-gamma and gamma-neutron combinations were obtained.

4.1 Data acquisition

The data used in this work were collected during an on-beam experiment at the Heavy Ion Laboratory (HIL), University of Warsaw, Poland. Nine NEDA detectors were placed 450 mm from the target centre at the 78-degree ring (theta angle measured with respect to the beam direction) of the EAGLE array [36]. Neutrons and gamma rays registered in NEDA detectors were produced by 171 MeV ^{32}S beam impinging on 0.75 mg/cm^2 ^{148}Sm target.

Signals from the NEDA detectors were read out by Caen V1725SB digitiser (250 MHz, 14 bit), independently from each other, when a CFD threshold (implemented in FPGA) was passed. Linear FIFO modules protected the digitiser against too large signals (above the Vpp range). CoMPASS software by CAEN installed on a server with Centos07 was used to read the digitiser via optical fibre.

4.2 Analysis and dataset generation

After the acquisition, the events were filtered by selecting only signals without pile-up. Later, classification between gammas and neutrons was carried out. Typically, in NEDA experiments, the offline analysis is performed using information from the TOF and CC ratio. However, the TOF information was unavailable in our case, so the NGD was based only on the CC information.

The CC is used to discriminate between neutron and gamma signals by analysing the shape of their pulses [37]. It is based on the ratio between two integration regions, shown in Fig. 4. This ratio of the integral value of the slow part of the pulse to the integral value of the fast interval is used to distinguish between the two types of signals. The following expression is used to determine whether it is a neutron or not:

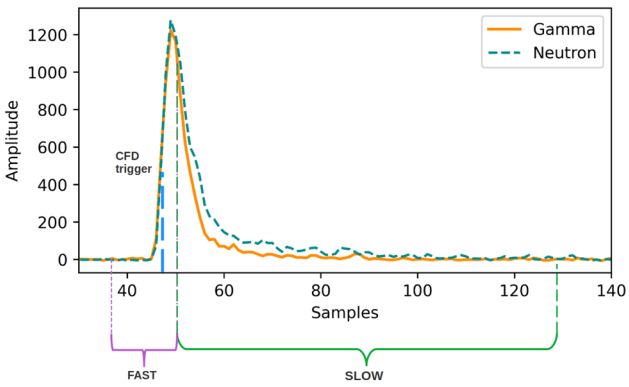

Fig. 4 Example of slow and fast interval in a single pulse

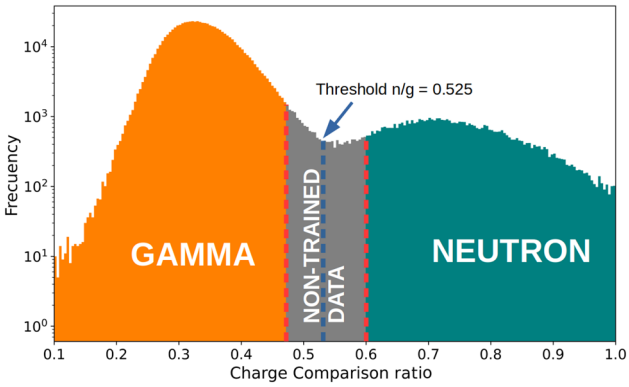

Fig. 5 (Colour online) Included and excluded events for training

$$\text{Is a neutron if} : \hat{I}_s > \hat{I}_\delta \cdot \hat{I}_f \tag{2}$$

where $\hat{I}_s$ the integral of the slow component of the input signal, $\hat{I}_f$ is the integral of the fast component, and the $\hat{I}_\delta$ is the discrimination threshold parameter.

Once the CC was applied to all the acquired signals, they were classified by particle type: gamma if the CC ratio is less than 0.525 and neutron if the result is greater, as shown in Fig. 5.

The threshold value was applied by observing where the lowest point in the valley between the gamma and neutron groups was located. Still, there may be neutrons with CC ratio lower than the threshold and gammas with values higher than the threshold. A more in-depth analysis of the events would also require information from the TOF. Since the TOF information was unavailable, the events closest to the threshold (neutron-gamma discrimination value) were not used to train the 1D-CAE. As shown in Fig. 5, events with a CC ratio in the range between 0.475 and 0.6 were not taken. Thus, events where the CC gives a value close to 0.525 were discarded for training. However, for the test dataset, events in this range were not discarded for the creation of artificial pile-up signals. The reason is that, during the

experiments, pile-up signals may be formed by pulses whose CC ratio is unknown, and the values may be in this range.

After classification, one signal of each type was taken, and one was shifted between 3 and 40 samples. In the case of Caen V1725SB digitiser, each sample is equivalent to 4 ns, so one of the two signals was shifted between 12 and 160 ns. Finally, both signals were added to generate a pile-up signal, as shown in Fig. 1.

Following this procedure, train and test datasets were generated with the same number of events. Each dataset contained 10,000 events generated with each delay, thus obtaining 380,000 neutron-gamma and 380,000 gamma-neutron combinations (760,000 events in each dataset). Also, the events were of different amplitudes from 150 to 7000 ADC counts, i.e. from 18 to 855 mV, to reconstruct pile-up events in the whole amplitude range of the acquisition.

The training dataset was used to train the 1D-CAE model, and the test dataset was used to test the model with unknown pile-up signals. The results of these tests are shown below.

5 Analysis of reconstructed signals for NEDA

Once the 1D-CAE model was trained, the test dataset (unknown signals to the system) was used, and the reconstructed pulses were evaluated, comparing them with the original pulses. The neutron or gamma pulse, the distance between pulse peaks, and the two possible combinations (gamma-neutron and neutron-gamma) were considered for evaluation.

The pile-up signals from the training dataset have been introduced into the 1D-CAE model, obtaining the two reconstructed pulses from which each input pile-up signal is formed. Finally, a CC analysis was carried out on these reconstructed pulses. Figure 6 shows an example of the reconstruction of pulses of pile-up signals.

As described in Sect. 2, neutron-gamma discrimination is crucial for the NEDA detector, and the CC method was used for this purpose. So, this analysis aims to verify that the expected particle type was obtained after reconstructing a pile-up event.

In the case of gamma rays, it was considered a success in the reconstruction when the CC ratio of the reconstructed pulse was lower than the neutron-gamma discrimination threshold (0.525). Figure 7 shows the distribution of the CC ratio of original gammas and the distribution of the CC ratio of reconstructed gammas. Comparing the two distributions, we found a mean value for the CC ratio of the original gammas of 0.34, whereas for the reconstructed gammas is 0.40. For the standard deviation, we obtain 0.072 for original gammas and 0.15 for reconstructed ones. Regarding the number of pulses identified correctly on the same side of the threshold, we have that 84.7% of the pulses that originally (without pile-up) would be classified as gamma rays would also be classified as gammas if present in a pile-up event.

For neutron reconstruction, if the CC ratio of the reconstructed signal was higher than the neutron-gamma discrimination threshold value (0.525), the event was considered a successful neutron. Figure 8 shows the CC distribution of the original neutrons and the CC distribution of the reconstructed neutrons. In this case, the mean values for the original and reconstructed neutron events are 0.73 and 0.67, respectively. For the standard deviation, we have 0.112 for the original neutrons and 0.181 for the ones after reconstruction. Again, the number of correctly identified neutrons after reconstruction is 83.3%.

From these results the confusion matrix is shown in Table 1.

As mentioned in Sect. 2, neutron-gamma and gamma-neutron are particle combinations that can give rise to pile-up events. These combinations can occur with different distances between pulses. Therefore, the results were analysed

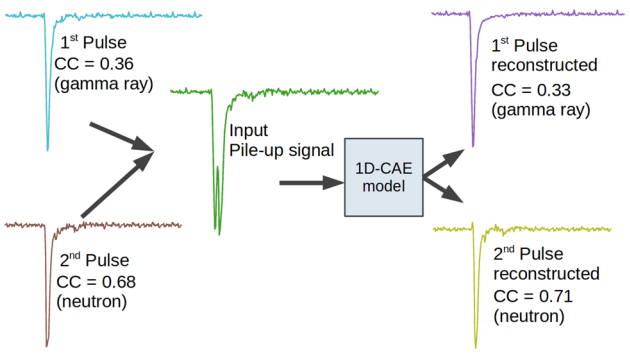

Fig. 6 Example of pile-up reconstruction

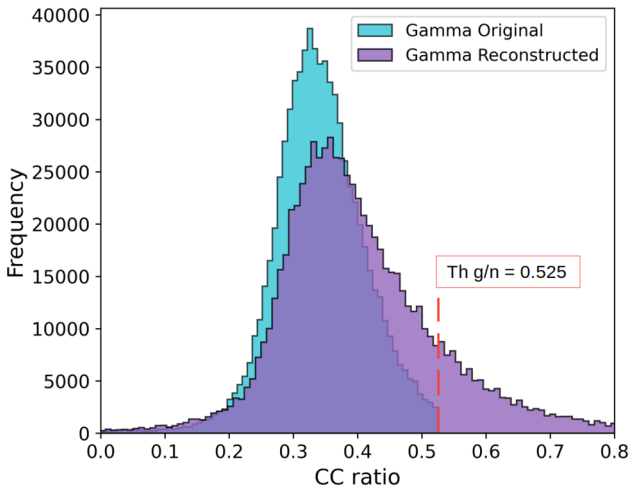

Fig. 7 (Color online) Distribution of CC ratio for the original gammas (without pile-up) and reconstructed gammas from pile-up events

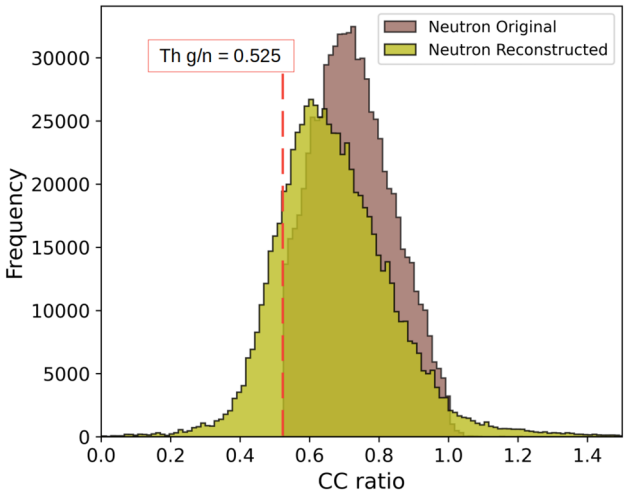

Fig. 8 (Color online) Distribution of CC ratio for the original neutrons (without pile-up) and reconstructed neutrons from pile-up events

Table 1 Confusion matrix of neutron and gamma reconstruction

	Neutron reconstructed (%)	Gamma reconstructed (%)
Neutron original	83.3	16.7
Gamma original	15.3	84.7

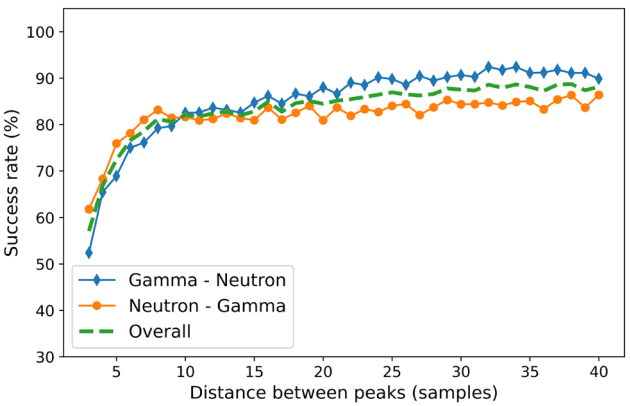

Fig. 9 (Color online) Percentage of success by distance between peaks

more profoundly considering the type of pile-up combination and the distance between pulses.

On the one hand, the success rate was studied after obtaining the ratio of CC of each reconstructed pulse for each distance between pulses and both combinations, as shown in Fig. 9. It can be seen that when the time distance is small in the gamma-neutron combination, the gammas are very close to the neutrons. This quasi-overlap makes the pile-up signal very similar to having a neutron without a pile-up. Therefore, in some cases, the first pulse was reconstructed in a way that was more similar to a neutron than to a gamma. On the contrary, when the time distance is longer in the neutron-gamma combination, the slower de-excitation of the neutron produced a tail with greater amplitude. This tail distorted the gamma signal more significantly, leading to a worse reconstruction of the gamma than in the gamma-neutron combination, where the gammas de-excited faster, distorting the second pulse (neutron) less.

Table 2 Confusion matrix of neutron-gamma and gamma-neutron reconstruction

	N-G reconstructed (%)	G-N reconstructed (%)
N-G original	83.95	16.05
G-N original	14.72	85.28

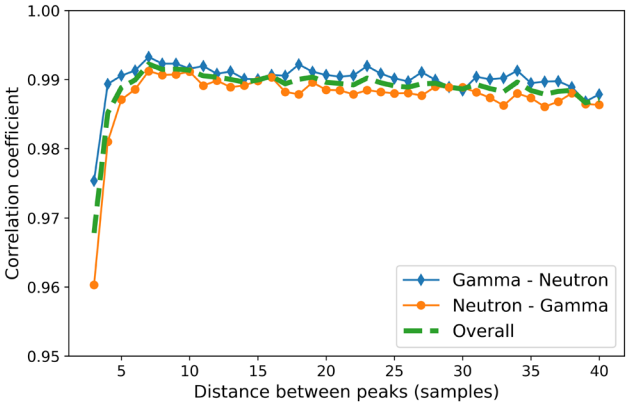

Fig. 10 Average correlation per delay

An 85.28% success rate was obtained for the gamma-neutron combination and an 82.61% success rate for the neutron-gamma combination. On average, 83.95% of the pulses were reconstructed, obtaining the same type of particle as the original events without pile-up.

From these results the confusion matrix is shown in Table 2.

On the other hand, we also analysed the correlation coefficient of the reconstructed signal shapes compared to the original signals. The mean correlation obtained was 0.988. Figure 10 shows the average correlation for each combination and each distance between pulses. Additionally, we calculated the *p-value* for all events, obtaining a mean *p-value* of 6.76×10^{-15}.

6 Conclusion

In summary, this research provides a strong solution to the common problem of pulse pile-up in nuclear spectroscopy, mainly focusing on the signals collected in NEDA experiments. The new method introduced in this study uses a 1D-CAE architecture, which relies on an autoencoder using 1D-CNN layers to reconstruct pile-up events effectively.

The evaluation of this method shows a high success rate of 83.95% in accurately reconstructing pile-up events, demonstrating its effectiveness in preserving important information. This means pile-up events previously ignored in NEDA can now be reconstructed and included in the analysis process. It is also worth noting that the reconstructed signals show a high average correlation of 0.988 compared to the original signals and a low *p-value* of 6.76×10^{-15}.

In order to address the pile-up problem, the limitations inherent in NEDA events have been considered, such as the need for a time difference of 15 ns or more between pulses and the requirement for low computational complexity. Therefore, this method offers a practical and efficient solution for processing signals in real time in future upgrades of NEDA electronics. This study not only provides a technical solution to the challenging problem of pulse pile-up but also emphasises the potential of the proposed 1D-CAE method as a practical and reliable tool for improving the accuracy and efficiency of nuclear spectroscopy experiments, especially those involving NEDA detectors.

Acknowledgements We acknowledge the HIL University of Warshaw facility for providing the heavy-ion beams and its technical staff for the support. We acknowledge the EAGLE and NEDA collaborations for the instrumental support.

Declarations

Conflict of interest The authors declare that they have no conflict of interest.

References

1. G.F. Knoll, *Radiation Detection and Measurement* (Wiley, New York, 2010)
2. M. Nakhostin, *Signal Processing for Radiation Detectors* (Wiley, New York, 2017)
3. X. Fabian, G. Baulieu, L. Ducroux et al., Artificial neural networks for neutron/ discrimination in the neutron detectors of neda. Nucl. Instrum. Methods Phys. Res. A **986**, 164750 (2021). https://doi.org/10.1016/J.NIMA.2020.164750
4. M.A. Nelson, B.D. Rooney, D.R. Dinwiddie et al., Analysis of digital timing methods with BaF_2 scintillators. Nucl. Instrum. Methods Phys. Res. A **505**, 324–327 (2003). https://doi.org/10.1016/S0168-9002(03)01078-7
5. Z. Gu, D.L. Prout, R. Taschereau et al., A new pulse pileup rejection method based on position shift identification. IEEE Trans. Nucl. Sci. **63**, 22–29 (2016). https://doi.org/10.1109/TNS.2015.2495169
6. M. Capogni, A. Ceccatelli, P.D. Felice et al., Random-summing correction and pile-up rejection in the sum-peak method. Appl. Radiat. Isot. **64**, 1229–1233 (2006). https://doi.org/10.1016/J.APRADISO.2006.02.027
7. J. Yu, J. Zhou, Y. Liu et al., Pile-up pulse continuous zone reject method. Appl. Radiat. Isot. **165**, 109319 (2020). https://doi.org/10.1016/j.apradiso.2020.109319
8. V.T. Jordanov, *Pile-Up Rejection Using Pulse-Shape Discrimination* (IEEE, New York, 2018), pp.1–4. https://doi.org/10.1109/NSSMIC.2018.8824551
9. E. Ronchi, P.A. Söderström, J. Nyberg et al., An artificial neural network based neutron-gamma discrimination and pile-up rejection framework for the BC-501 liquid scintillation detector. Nucl. Instrum. Methods Phys. Res. A **610**, 534–539 (2009). https://doi.org/10.1016/j.nima.2009.08.064
10. P. Bastia, G. Bertuccio, F. Borghetti et al., An integrated reset/pulse pile-up rejection circuit for pixel readout asics. IEEE Trans. Nucl. Sci. **53**, 414–417 (2006). https://doi.org/10.1109/TNS.2006.869852
11. W. Guo, S.H. Lee, R.P. Gardner, The Monte Carlo approach MCPUT for correcting pile-up distorted pulse-height spectra. Nucl. Instrum. Methods Phys. Res. A **531**, 520–529 (2004). https://doi.org/10.1016/J.NIMA.2004.05.089
12. L. Sabbatucci, V. Scot, J.E. Fernandez, Multi-shape pulse pile-up correction: the MCPPU code. Radiat. Phys. Chem. **104**, 372–375 (2014). https://doi.org/10.1016/J.RADPHYSCHEM.2014.04.034
13. M.R. Mohammadian-Behbahani, S. Saramad, A comparison study of the pile-up correction algorithms. Nucl. Instrum. Methods Phys. Res. A **951**, 163013 (2020). https://doi.org/10.1016/J.NIMA.2019.163013
14. C. Yi, J. Han, R. Song et al., Discrimination of piled-up neutron-gamma pulses using charge comparison method and neural network for CLYC detectors. Nucl. Instrum. Methods Phys. Res. A **1055**, 168561 (2023). https://doi.org/10.1016/J.NIMA.2023.168561
15. I. Morad, M. Ghelman, D. Ginzburg et al., Model-based deep learning algorithm for pulse shape discrimination in high event rates. EPJ Web Conf. **288**, 10001 (2023). https://doi.org/10.1051/EPJCONF/202328810001
16. S. Peng, Z. Hua, Q. Wu et al., Piled-up neutron-gamma discrimination system for CLLB using convolutional neural network. J. Instrum. **17**, T08001 (2022). https://doi.org/10.1088/1748-0221/17/08/T08001
17. S. Marrone, D. Cano-Ott, N. Colonna et al., Pulse shape analysis of liquid scintillators for neutron studies. Nucl. Instrum. Methods Phys. Res. A **490**, 299–307 (2002). https://doi.org/10.1016/S0168-9002(02)01063-X
18. F. Belli, B. Esposito, D. Marocco et al., A method for digital processing of pile-up events in organic scintillators. Nucl. Instrum. Methods Phys. Res. A **595**, 512–519 (2008). https://doi.org/10.1016/J.NIMA.2008.06.045
19. M.E. Hammad, H. Kasban, R.M. Fikry et al., Pile-up correction algorithm for high count rate gamma ray spectroscopy. Appl. Radiat. Isot. **151**, 196–206 (2019). https://doi.org/10.1016/J.APRADISO.2019.06.003
20. W. Guo, R.P. Gardner, C.W. Mayo, A study of the real-time deconvolution of digitized waveforms with pulse pile up for digital radiation spectroscopy. Nucl. Instrum. Methods Phys. Res. A **544**, 668–678 (2005). https://doi.org/10.1016/J.NIMA.2004.12.036
21. X.L. Luo, V. Modamio, J. Nyberg et al., Pulse pile-up identification and reconstruction for liquid scintillator based neutron detectors. Nucl. Instrum. Methods Phys. Res. A **897**, 59–65 (2018). https://doi.org/10.1016/J.NIMA.2018.03.078

22. C. Fu, A.D. Fulvio, S.D. Clarke et al., Artificial neural network algorithms for pulse shape discrimination and recovery of piled-up pulses in organic scintillators. Ann. Nucl. Energy **120**, 410–421 (2018). https://doi.org/10.1016/J.ANUCENE.2018.05.054
23. J.J. Valiente-Dobón, G. Jaworski, A. Goasduff et al., NEDA - NEutron Detector Array. Nucl. Instrum. Methods Phys. Res. A **927**, 81–86 (2019). https://doi.org/10.1016/j.nima.2019.02.021
24. S. Kiranyaz, O. Avci, O. Abdeljaber et al., 1D convolutional neural networks and applications: a survey. Mech. Syst. Signal Pr. **151**, 107398 (2021). https://doi.org/10.1016/J.YMSSP.2020.107398
25. D. Bank, N. Koenigstein, R. Giryes, *Autoencoders* (Springer, Cham, 2023), pp.353–374. https://doi.org/10.1007/978-3-031-24628-9_16
26. Z. Li, F. Liu, W. Yang et al., A survey of convolutional neural networks: analysis, applications, and prospects. IEEE Trans. Neural Netw. Learn. Syst. **33**, 6999–7019 (2022). https://doi.org/10.1109/TNNLS.2021.3084827
27. U. Erdenebayar, H. Kim, J.U. Park, et al., Automatic prediction of atrial fibrillation based on convolutional neural network using a short-term normal electrocardiogram signal. J. Korean Med. Sci. **34**, e64 (2019) https://doi.org/10.3346/JKMS.2019.34.E64
28. S. Mehrkanoon, Deep shared representation learning for weather elements forecasting. Knowl.-Based Syst. **179**, 120–128 (2019). https://doi.org/10.1016/J.KNOSYS.2019.05.009
29. L. Deng, X. Li, Machine learning paradigms for speech recognition: An overview. IEEE ACM Trans. Audio Speech Lang. Process. **21**, 1060–1089 (2013). https://doi.org/10.1109/TASL.2013.2244083
30. P. Li, Y. Pei, J. Li, A comprehensive survey on design and application of autoencoder in deep learning. Appl. Soft Comput. **138**, 110176 (2023). https://doi.org/10.1016/J.ASOC.2023.110176
31. R. Ranjan, V.M. Patel, R. Chellappa, Hyperface: a deep multi-task learning framework for face detection, landmark localization, pose estimation, and gender recognition. IEEE Trans. Pattern Anal. Mach. Intell. **41**, 121–135 (2019). https://doi.org/10.1109/TPAMI.2017.2781233
32. D.P. Kingma, M. Welling, Auto-encoding variational bayes, in *2nd International Conference on Learning Representations, ICLR 2014—Conference Track Proceedings*
33. P. Vincent, H. Larochelle, Y. Bengio, et al., Extracting and composing robust features with denoising autoencoders, in *Proceedings of the 25th International Conference on Machine Learning* (2008), pp. 1096–1103. https://doi.org/10.1145/1390156.1390294
34. Versal adaptive socs. https://www.amd.com/en/products/adaptive-socs-and-fpgas/versal.html#overview
35. STM32l4 - arm cortex-m4 ultra-low-power mcus - stmicroelectronics. https://www.st.com/en/microcontrollers-microprocessors/stm32l4-series.html
36. J. Mierzejewski, J. Srebrny, H. Mierzejewski et al., EAGLE-the central European Array for Gamma Levels Evaluation at the Heavy Ion Laboratory of the University of Warsaw. Nucl. Instrum. Methods Phys. Res. A **659**, 84–90 (2011). https://doi.org/10.1016/j.nima.2011.08.037
37. A. Raggio, G. Jaworski, V. Modamio, et al., Pulse shape analysis of the NEDA detector. LNL Anual Report 98–99 (2016)